This is the final author version of

M. K. T. Al-Nuaimi, W. Hong, and W. G. Whittow, "Aperiodic Sunflower Like Metasurface for Diffusive Scattering and RCS Reduction," IEEE Antennas Wirel. Propag. Lett., pp. 1–1, 2020.

The DOI is: 10.1109/LAWP.2020.2980906

The paper can also be downloaded here

https://ieeexplore.ieee.org/document/9037099

More than 70 other academic journal papers by Dr. Whittow can be freely downloaded here:

http://publications.lboro.ac.uk/publications/all/collated/elwgw.html

Aperiodic Sunflower Like Metasurface for Diffusive Scattering and RCS Reduction

Mustafa K. Taher Al-Nuaimi, Wei Hong, Fellow, IEEE, William G. Whittow, Senior Member, IEEE

***Abstract*— This article presents the design of aperiodic sunflower-like metasurface for circularly polarized (CP) wave diffusion and radar cross section (RCS) reduction using Pancharatnam-Berry (PB) meta-atoms. The distribution of the PB meta-atoms across the metasurface aperture is non-uniform and has a distribution inspired by sunflower seeds, i.e., an outwardly logarithmic spiral lattice with no transitional periodicity. The proposed metasurface has 600 PB meta-atoms of sub-wavelength size of 5 mm ≈ $0.33\lambda_{20GHz}$ and exhibits a randomly chosen diffusive reflection phase between 0^o and 360^o. Both simulated and experimental results demonstrate that the proposed sunflower-like metasurface can efficiently diffuse the backscattered energy into numerous directions when normally illuminated by a CP-wave with RCS reduction > 7 dB between 16 GHz and 23.8 GHz. Furthermore, the low-level diffuse scattering can be preserved under oblique incidence up to 60^o. As a result of using this PB concept, the polarization sensitivity of the proposed metasurface is released and this is highly desired in applications when the polarization of the incoming wave is unknown.**

***Index Terms*— metasurface, diffuse reflection, reflective surface, reflectarray.**

I. Introduction

Manipulation of electromagnetic waves using metasurfaces has been a hot topic in recent years [1]-[8]. Electromagnetic wave (EM-wave) diffusion and radar cross section (RCS) reduction is one of the applications of metasurface [9]-[12]. Metasurfaces are the 2D version or counterparts of metamaterials which are usually constituted by an array of periodic or non-periodic sub-wavelength metallic or dielectric resonators [13]-[14]. In [2]-[8], a chessboard and checkerboard like metasurfaces for RCS reduction were proposed using two kinds of meta-atoms exhibiting an $180^o \pm 25^o$ phase difference between their absolute reflection phases. However, such kind of surfaces suffers from strong scattering in certain directions and degraded scattering characteristics under oblique incidence. In [1] a modified chessboard was proposed, and each quadrant of the conventional chessboard was replaced by a small size 1-bit reflectarray exhibiting an optimized diffusive 1-bit quantized phase distribution to achieve nearly uniform diffusive scattering under both normal and oblique incidence of EM-waves. In [10]-[11], the scattering characteristics of metasurfaces exhibiting concave and convex reflection phases were investigated for RCS reduction for linearly polarized waves. Furthermore, a coding metasurface was introduced in [15]-[16] in which the coding particles (unit cells) were arranged according to a certain coding sequence to achieve low-level backscattering, and potentially any other desired functions [17]-[20]. In [1]-[20], metasurfaces were designed by placing meta-atoms and scatterers in rectangular periodic grids (framework). Important questions include whether this periodic arrangement is always the best option and whether it is possible to design metasurfaces with aperiodic distribution of meta-atoms to achieve elegant diffusion characteristics for circularly polarized (CP) waves.

In this letter, the design of aperiodic sunflower-like metasurfaces for CP-wave diffusion and RCS reduction using Pancharatnam-Berry (PB) meta-atoms is presented. The distribution of the PB meta-atoms across the metasurface aperture is non-uniform and has a sunflower seed inspired distribution, i.e., outwardly logarithmic spiral lattice of no transitional periodicity. All PB meta-atoms exhibit a randomly chosen diffusive reflection phase between 0^o and 360^o. Both simulated and experimental results demonstrate that the proposed sunflower-like metasurface can efficiently diffuse the backscattered energy with RCS reduction of a metallic plate.

II. PB Meta-Atom Design

The geometry of the proposed anisotropic sub-wavelength PB meta-atom is presented in Fig. 1 (a) and (b) and consists of a copper resonator of dumbbell-shape etched on the upper side of a dielectric spacer (ε_r=4.4, h=2 mm) and backed by copper ground, the thickness of the copper film is 0.018 mm. The frequency-domain solver of the CST Microwave Studio has been used to obtain the reflection characteristics of the unit cell via conducting a series of electromagnetic numerical simulations [21]-[22]. For the purpose of achieving high efficiency PB meta-atoms, the dimensions of the metallic resonator have been optimized and final dimensions of the anisotropic PB meta-atom are: W=0.3, P=5, R=0.6 (all in mm). When the proposed PB meta-atom was illuminated by a CP wave, it has a high co-polarization (co-pol) reflection and very low cross-

Manuscript received March XX, XXXX; revised March XX, XXXX; accepted March XX, XXXX. Date of publication March XX, XXXX; date of current version March XX, XXXX. This work was part supported by EPSRC grant: 'ANISAT', EP/S030301/1. Corresponding author: M. K. T. Al-Nuaimi.

M. K. T. Al-Nuaimi formerly was with the State Key Laboratory of Millimeter Waves, Southeast University, Nanjing 210096, China (e-mail: mustafa.engineer@yahoo.com).

Wei Hong and Zhang-Cheng Hao are with the School of Information Science and Engineering, Southeast University, Nanjing, 210096, P. R. China.

W. G. Whittow is with Wolfson School of Mechanical, Electrical and Manufacturing Engineering, Loughborough University, Loughborough LE11 3TU, U.K.

Digital object identifier XX.XXXX/AWPL.XX.XX.2020

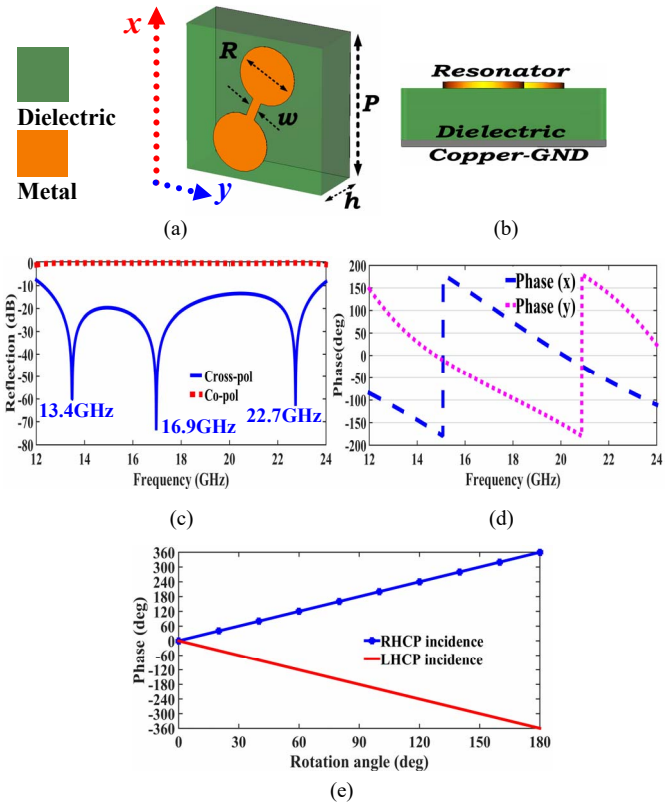

Fig. 1. Geometry and simulated results (a) and (b) are sketches of the PB unit cell. (c) co-pol and cross-pol reflection coefficients under CP incident wave. (d) Reflection phase of the unit cell under illumination of x- and y-polarized plane waves. (e) Reflection phase versus rotation angle of the unit cell when illuminated by LHCP and RHCP waves.

polarization (cross-pol) reflection as can be seen in Fig. 1 (c). The reflection phase of this PB meta-atom when illuminated by x- or y-polarized waves, respectively, is presented in Fig. 1 (d). As can be seen the reflection phase is continuous and there is about $180^o \pm 27^o$ phase difference between x- and y-polarized reflections between 14.1 GHz and 23.3 GHz. According to PB phase theory [9], [23], if the unit cell has a high reflection magnitude under LP wave illumination with around 180^o reflection phase difference between orthogonal linearly x- and y- polarized incidences. Then when the unit cell is illuminated by a CP wave the cross-pol reflection will be significantly reduced, leading to high co-pol reflection. In addition to, co-pol reflection phase (φ) can be expressed as $\varphi=\pm 2\psi$, where the polarization sign "–" and "+" corresponds to LHCP and RHCP incident waves, respectively, and ψ is the rotation angle of the dumbbell-shape metallic resonator. Based on the angular rotation of the copper resonator, a 360^o co-pol reflection phase is achieved as shown in Fig. 1 (e) when the angular rotation angle increased gradually from 0^o to 180^o.

III. Sunflower Like CP Metasurface Design

The PB meta-atoms of proposed sunflower-like CP metasurface should be arranged in similar way to the seeds of a sunflower in nature as shown in Fig. 2 (a). In other words, realizing a logarithmic spiral lattice. The position of each PB meta-atom in the xy-plane can be found using eq. (1) which is

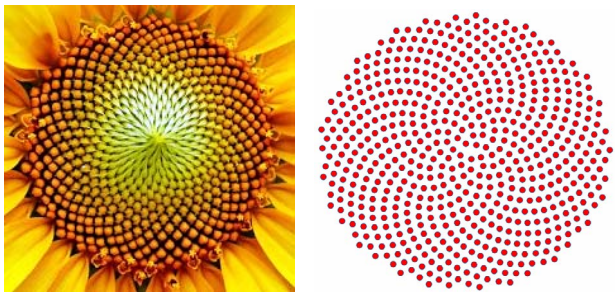

Fig. 2. (a) Sunflower in nature [24] and (b) PB meta-atoms distribution calculated using eq. (1).

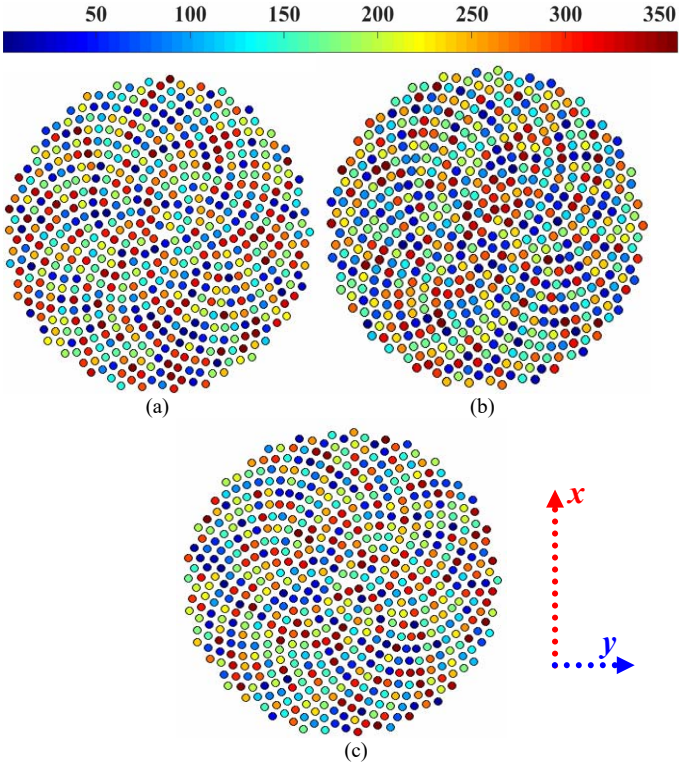

Fig. 3. Reflection phase distribution of the three sunflower-like metasurfaces: (a) SFM#1, (b) SFM#2, (c) SFM#3. All surfaces have N=600, D=142mm.

$$X_c = \sqrt{\frac{S^2 \times n}{\pi}} \times \cos(2\pi n\tau), \quad Y_c = \sqrt{\frac{S^2 \times n}{\pi}} \times \sin(2\pi n\tau) \tag{1}$$

the Cartesian form of the polar equations in [25]-[27]. In eq. (1), τ is the spiral golden ratio, S is the spacing between the centers of any two adjacent meta-atoms, n is the number of meta-atom on the metasurface aperture (n=1,…., N, where N is the total umber of meta-atoms). Using MATLAB code, the positions of the PB meta-atoms were calculated using eq. (1) as shown in Fig.2 (b) for S=5 mm, $\tau = (\sqrt{5}+1)/2$, and N=600. As can be seen in such an aperiodic distribution, the meta-atoms are not too far from each other and at the same time not overlapping.

The required diffusive reflection phase at each unit cell should be calculated such that the backscattered energy will be distributed in a nearly uniform shape in the half space in front of the sunflower-like CP metasurface. A random diffusive phase (DP) between 0^o and 360^o was introduced for each PB meta-atom of the metasurface by rotating the metallic resonators by a certain angle (ψ) based on the PB formula

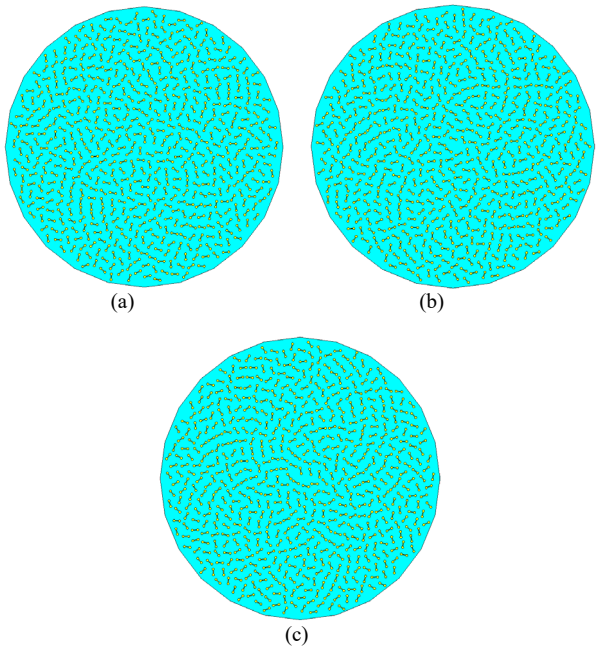

Fig. 4. Layout of the sunflower like metasurfaces to achieve the required phase distributions : (a) SFM#1, (b) SFM#2, (c) SFM#3. All surfaces have N=600, D=142mm.

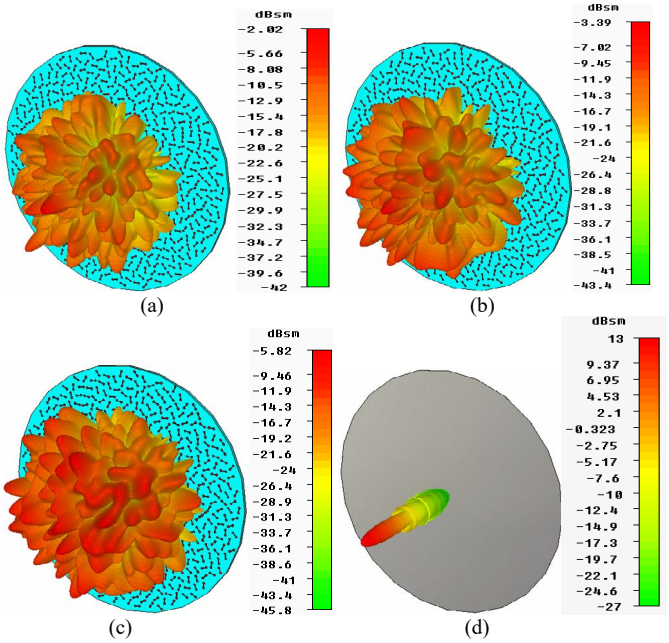

Fig. 5. Simulated far-field Scattering patterns of the sunflower like metasurfaces feom CP-wave at normal incidence: (a) SFM#1, (b) SFM#2, (c) SFM#3, and (d) PEC plate.

DP=2ψ. The random phase distribution of the whole sunflower metasurface was generated by a random function produced by MATLAB. Three different random phase distribution maps are shown in Fig.3 and named as SFM#1, SFM#2, and SFM#3, respectively. It is important here to mention that each phase distribution map leads to different phase distributions and different scattering patterns. Based on the phase distribution maps, three diffusive metasurfaces are designed as shown in Fig. 4 and the metasurfaces have ultra-thin thickness of 0.12λ. The time-solver of CST Microwave Studio was used to obtain the diffusion characteristics of these metasurfaces. The 3D far-field

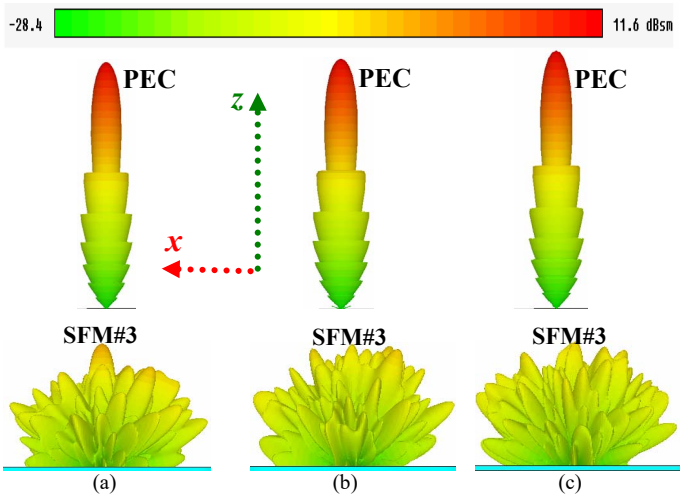

Fig. 6. Simulated 3D far-field scattering patterns of PEC plate (top) and the sunflower like metasurface SFM#3 (bottom) at: (a) 18 GHz, (b) 19 GHz, (c) 20 GHz.

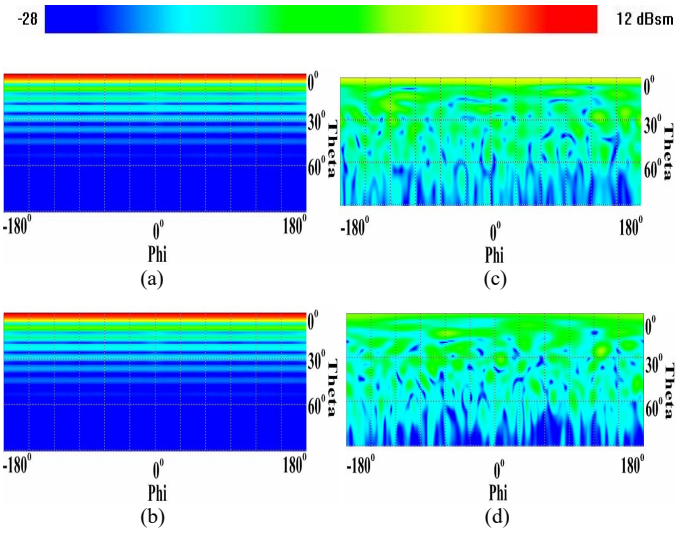

Fig. 7. 2D backscattered field distribution (a) and (b) for PEC plate, (c) and (d) for SFM#3 at 19 GHz (top) and 20 GHz (bottom).

scattering patterns of the three sunflower-like metasurfaces under normal illumination of CP plane wave are presented in Fig.5. The scattering patterns of all three sunflower-like metasurfaces have a diffuse-like scattering patterns at all frequencies and it is very obvious that the specular reflection wave front has been destroyed which is intrinsically different from that of a equal-sized PEC plate in Fig.5 (d) for which the specular reflection according to Snell's law of reflection is dominated. As a result of the phase change across the metasurface aperture and the aperiodic distribution of PB meta-atoms, the incident wave is reflected in countless directions (angles) in the whole half space in front of the three metasurfaces. Its was observed that the sunflower-like metasurface (SFM#3) in Fig.5 (c) had the lowest scattering levels and exhibited much more uniform scattering patterns. The scattering patterns of SFM#3 at various frequencies are presented in Fig. 6 which shows that a low-level diffused scattering pattern dominates compared with those of equal-sized PEC plates at the same frequencies for which a single beam specular reflection is dominated. To more

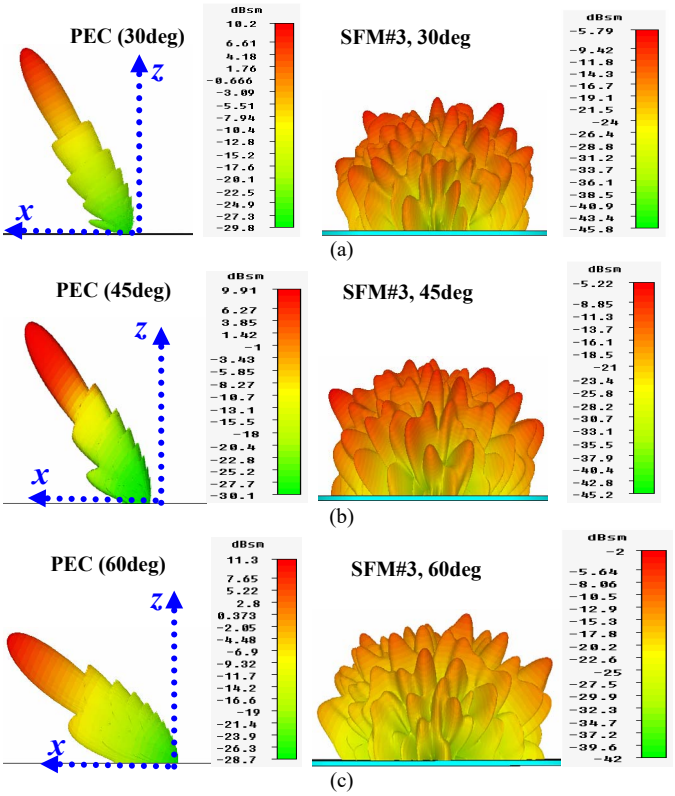

Fig. 8. Simulated scattering characteristics of SFM#3 under oblique incidence of CP-wave when θ_{inc} is (a) 30°, (b) 45°, and (c) 60°.

understand the scattering characteristics of SFM#3, the 2D backscattered field distribution is presented in Fig.7 and as can be seen the backscattered field is diffused and distributed on the half space in front of SFM#3 which is not the case for a PEC plate in which the backscattered field is very strong in the boresight direction for all phi angles. The diffuse scattering characteristics of SFM#3 under oblique incidence of CP wave are also investigated and the results are presented in Fig. 8. Here three cases are considered when the incident angle (θ_{inc}) is 30°, 45°, and 60°. As can be seen, even under the illumination of oblique CP wave the sunflower metasurface still efficiently diffuse the incident CP wave.

IV. Fabrication and Measurements

For experimental verification of the proposed CP sunflower-like metasurface, SFM#3 was fabricated using the standard printed circuit board (PCB) process as shown in Fig. 9 (a). The reflection measurements were performed inside an anechoic chamber to reduce the reflections and interferences from the surroundings. The measurement setup is shown in Fig. 9 (b). In the measurement setup, a pair of horn antenna serving as transmitter (T_x) and receiver (R_x) are connected to a vector network analyzer via coaxial cables. The distance between the horn antennas and the SFM#3 under test was chosen carefully according to far-field formula in [28]. To avoid unwanted reflections from nearby objects, the time gating function of the VNA was used. The simulated and measured RCS curves of both SFM#3 and a bare copper plate are presented in Fig. 9 (c). Greater than 7-dB reduction was achieved across the band from 16 GHz to 23.8 GHz with approximately 18 dB reduction around 20 GHz. The small deviation between the measured and simulated RCS results in Fig. 9 (c) can be attributed to the

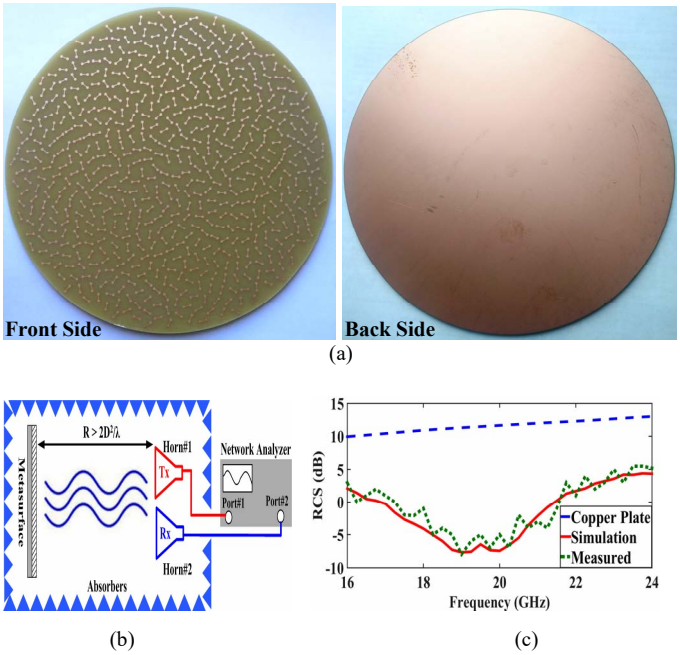

Fig. 9. (a) Photographs of the fabricated SFM#3. (b) The measurement setup inside anechoic chamber. (c) Measured RCS of SFM#3 and a copper plate.

misalignment of the horn antennas and the metasurfaces inside the anechoic chamber during the measurements, the fabrication error, and the uncertainty of the dielectric permittivity of the substrate at this frequency.

It is well known that the conventional chessboard metasurface suffers from strong scattering in certain directions and degraded scattering characteristics under oblique incidence. The modified chessboard structure in [1] consists a four reflectarrays and using 1-bit quantized parabolic reflection phase. In other words, only two phase states (0° and 180°) were used. Also, in [1] the unit cells have been distributed periodically in rectangular grids. Compared to those chessboard metasurfaces in the literature, the proposed SFM#3 has a countless number of random PB phase states between 0° and 360° and an aperiodic distribution of PB meta-atoms across its aperture. Compared to the RCS patterns in [1], its been noticed that for the proposed surface the backscattered energy is severely diffused and distributed in a more uniform fashion in front of SFM#3 as shown in Fig. 5. Furthermore, the proposed sunflower-like metasurface has a lower RCS scattering levels under oblique incidence compared to the modified chessboard in [1].

Conclusion

In summary, the proposed aperiodic SFM#3 uses Pancharatnam-Berry (PB) meta-atoms and the distribution of the 600 PB meta-atoms across the metasurface aperture is non-uniform and has a sunflower seed-like distribution with random reflection phase. Both simulated and experimental results demonstrated that the proposed sunflower-like metasurface can efficiently diffuse the backscattered energy into numerous directions when normally illuminated by a CP-wave. The RCS reduction was greater 7 dB across the frequency range 16 GHz to 23.8 GHz. Furthermore, the low-level diffuse scattering is preserved under oblique incidence up to 60°.

REFERENCES

[1] M. K. T. Al-Nuaimi, W. Hong and Y. He, "Design of Diffusive Modified Chessboard Metasurface," *IEEE Antennas and Wireless Propagation Letters*, vol. 18, no. 8, pp. 1621-1625, Aug. 2019.

[2] W. Chen, C. A. Balanis, C. R. Birtcher and A. Y. Modi, "Cylindrically Curved Checkerboard Surfaces for Radar Cross-Section Reduction," *IEEE Antennas and Wireless Propagation Letters*, vol. 17, no. 2, pp. 343-346, Feb. 2018.

[3] W. Chen, C. A. Balanis and C. R. Birtcher, "Checkerboard EBG Surfaces for Wideband Radar Cross Section Reduction," *IEEE Transactions on Antennas and Propagation*, vol. 63, no. 6, pp. 2636-2645, June 2015.

[4] W. Chen, C. A. Balanis and C. R. Birtcher, "Dual Wide-Band Checkerboard Surfaces for Radar Cross Section Reduction," *IEEE Transactions on Antennas and Propagation*, vol. 64, no. 9, pp. 4133-4138, Sept. 2016.

[5] J. Xue, W. Jiang and S. Gong, "Chessboard AMC Surface Based on Quasi-Fractal Structure for Wideband RCS Reduction," *IEEE Antennas and Wireless Propagation Letters*, vol. 17, no. 2, pp. 201-204, Feb. 2018.

[6] M. Mighani and G. Dadashzadeh, "Broadband RCS reduction using a novel double layer chessboard AMC surface," *Electronics Letters*, vol. 52, no. 14, pp. 1253-1255, 7 7 2016.

[7] K. Li, Y. Liu, Y. Jia and Y. J. Guo, "A Circularly Polarized High-Gain Antenna With Low RCS Over a Wideband Using Chessboard Polarization Conversion Metasurfaces," *IEEE Transactions on Antennas and Propagation*, vol. 65, no. 8, pp. 4288-4292, Aug. 2017.

[8] W. Chen, C. A. Balanis and C. R. Birtcher, "Dual Wide-Band Checkerboard Surfaces for Radar Cross Section Reduction," *IEEE Transactions on Antennas and Propagation*, vol. 64, no. 9, pp. 4133-4138, Sept. 2016.

[9] H. X. Xu, et.al, "Deterministic Approach to Achieve Broadband Polarization-Independent Diffusive Scatterings Based on Metasurfaces," ACS Photonics, vol.5, pp. 1691-1702, 2018.

[10] H. Xu, S. Ma, X. Ling, L. Zhou, H. Xu and X. Zhang, "Broadband Wide-Angle Polarization-Independent Diffusion Using Parabolic-Phase Metasurface," in Proceedings of 2018 IEEE International Symposium on Electromagnetic Compatibility and 2018 IEEE Asia-Pacific Symposium on Electromagnetic Compatibility (EMC/APEMC), pp. 1114-1118,Singapore, 2018.

[11] F. Yuan, H. Xu, X. Jia, G. Wang and Y. Fu, "RCS Reduction Based on Concave/Convex-Chessboard Random Parabolic-Phased Metasurface, " IEEE Transactions on Antennas and Propagation, 2019.

[12] X. Liu, J. Gao, L. Xu, X. Cao, Y. Zhao and S. Li, "A Coding Diffuse Metasurface for RCS Reduction," IEEE Antennas and Wireless Propagation Letters, vol. 16, pp. 724-727, 2017.

[13] M. K. T. Al-Nuaimi et. al., "Backscattered EM-wave manipulation using low cost 1-bit reflective surface at W-band," Journal of Physics D: Applied Physics, vol. 51, 2018.

[14] H. Sun, et. al. "Broadband and Broad-angle Polarization-independent Metasurface for Radar Cross Section Reduction," Scientific Reports, volume 7, Article number: 40782, 2017.

[15] T. J. Cui, M. Q. Qi, X. Wan, J. Zhao, and Q. Cheng, "Coding Metamaterials, Digital Metamaterials and Programmable Metamaterials," Light: Science and Applications 3, 2014.

[16] T. J. Cui, et. al., "Information Metamaterials and Metasurfaces," Journal of Materials Chemistry C 5, 2017.

[17] Y. Zhuang, "Design of bifunctional metasurface based on independent control of transmission and reflection", Optics Express, vol. 26, Issue 3, pp. 3594-3603, 2018.

[18] H. X. Xu, Haiwen Liu, Xiaohui Ling, Yunming Sun, and Fang Yuan, "Broadband Vortex Beam Generation Using Multimode Pancharatnam–Berry Metasurface," IEEE Transactions On Antennas And Propagation, Vol. 65, No. 12, 2017.

[19] H. X. Xu， et. al., " High-efficiency Broadband Polarization-Independent Superscatterer Using Conformal Metasurfaces," Photonics Research, vol. 6, No. 8, , 2018,

[20] N. F. Yu, et. al., "Light Propagation with Phase Discontinuities: Generalized Laws of Reflection and Refraction," Science 334, pp. 333–337, 2011.

[21] CST Microwave Studio: www.cst.com.

[22] M. K. T. Al-Nuaimi, W. Hong and A. Mahmoud, "Design of cross polarization conversion metasurface using dumbbell-like unit cell," *2017 Sixth Asia-Pacific Conference on Antennas and Propagation (APCAP)*, pp. 1-3, Xi'an, China, 2017.

[23] K. Chen, et al., "Geometric phase coded metasurface: from polarization dependent directive electromagnetic wave scattering to diffusion-like scattering," Scientific Reports, vol. 6, Article number: 35968, 2016.

[24] Website:http://polymath07.blogspot.com/2010/07/steps-on-spiral-staircase.html.

[25] M. W. Niaz, Z. Ahmed, M. B. Ihsan, "Reflectarray with logarithmic spiral lattice of elementary antennas on its aperture," *AEU - International Journal of Electronics and Communications*, 2016.

[26] D. W. Boeringer, "Phased array including a logarithmic spiral lattice of uniformly spaced radiation and receiving elements," *U. S. patent*, vol. B1, 2002.

[27] M. W. Niaz, Y. Yin, S. Zheng and J. Chen, "On the Design of Low Sidelobe Reflectarray with Enhanced Bandwidth at Ku-band," *2019 13th European Conference on Antennas and Propagation (EuCAP)*, Krakow, Poland, 2019.

[28] C. A. Balanis, Antenna Theory, Analysis and Design, 2nd edition, Wiley, New York, 1996.